Behavioral/Cognitive

Medial Frontal Cortex Activity Predicts Information Sampling in Economic Choice

Paula Kaanders,[1,2] **Hamed Nili,**[1,3] **Jill X. O'Reilly,**[1,2] **and Laurence Hunt**[1,4]

[1]Wellcome Centre for Integrative Neuroimaging, University of Oxford, Oxford OX3 9DU, England, [2]Department of Experimental Psychology, University of Oxford, Oxford OX2 6GG, England, [3]Nuffield Department of Clinical Neurosciences, University of Oxford, Oxford OX3 9DU, England, and [4]Department of Psychiatry, University of Oxford, Oxford OX3 7JX, England

Decision-making not only requires agents to decide what to choose but also how much information to sample before committing to a choice. Previously established frameworks for economic choice argue for a deliberative process of evidence accumulation across time. These tacitly acknowledge a role of information sampling in that decisions are only made once sufficient evidence is acquired, yet few experiments have explicitly placed information sampling under the participant's control. Here, we use fMRI to investigate the neural basis of information sampling in economic choice by allowing participants (n = 30, sex not recorded) to actively sample information in a multistep decision task. We show that medial frontal cortex (MFC) activity is predictive of further information sampling before choice. Choice difficulty (inverse value difference, keeping sensory difficulty constant) was also encoded in MFC, but this effect was explained away by the inclusion of information sampling as a coregressor in the general linear model. A distributed network of regions across the prefrontal cortex encoded key features of the sampled information at the time it was presented. We propose that MFC is an important controller of the extent to which information is gathered before committing to an economic choice. This role may explain why MFC activity has been associated with evidence accumulation in previous studies in which information sampling was an implicit rather than explicit feature of the decision.

Key words: **decision-making; fMRI; information sampling; prefrontal cortex**

Significance Statement

The decisions we make are determined by the information we have sampled before committing to a choice. Accumulator frameworks of decision-making tacitly acknowledge the need to sample further information during the evidence accumulation process until a decision boundary is reached. However, relatively few studies explicitly place this decision to sample further information under the participant's control. In this fMRI study, we find that MFC activity is related to information sampling decisions in a multistep economic choice task. This suggests that an important role of evidence representations within MFC may be to guide adaptive sequential decisions to sample further information before committing to a final decision.

Introduction

Decisions are determined by the information the decision-maker samples before committing to a choice. Since the 1970s, cognitive psychologists have developed ways to determine how participants decide to sample information as a decision unfolds (Newell and Simon, 1972; Payne, 1976). This has led to a rich understanding of the role of information sampling in economic choice behavior (Bettman et al., 1998; Hunt et al., 2016; Navarro et al., 2016; Stewart et al., 2016; Kobayashi et al., 2019).

Perhaps the most pervasive behavioral effect is that more difficult decisions, that is, when options are particularly close in value, take longer to make, potentially allowing more time for the agent to acquire information about the alternatives (Jamieson and Petrusic, 1977; Busemeyer and Townsend, 1993; Milosavljevic et al., 2010; Hunt et al., 2012). Evidence accumulation frameworks such as the drift diffusion model tacitly assume that more difficult decisions with longer reaction times are those in which more information is sampled (Usher and McClelland, 2001; Ratcliff and McKoon, 2008; Shadlen and Shohamy, 2016). Recent models have further argued that in economic choice, visual fixation provides a window into which option is currently being sampled, biasing evidence accumulation toward this attended option (Krajbich et al., 2010; Smith and Krajbich, 2019). However, the links among

Received Feb. 22, 2021; revised June 17, 2021; accepted Aug. 7, 2021.

Author contributions: P.K. and L.H. designed research; P.K. performed research; H.N. and J.X.O. contributed unpublished reagents/analytic tools; P.K., H.N., J.X.O., and L.H. analyzed data; P.K. and L.H. wrote the paper.

P.K. was supported by a Wellcome Trust Studentship (215350/Z/19/Z). J.X.O. was supported by a Career Development Award from the Medical Research Council (MR/L019639/1). L.H. was supported by a Sir Henry Dale Fellowship from the Wellcome Trust and the Royal Society (208789/Z/17/Z).

The authors declare no competing financial interests.

Correspondence should be addressed to Paula Kaanders at paula.kaanders@psy.ox.ac.uk or Laurence Hunt at laurence.hunt@psych.ox.ac.uk.

https://doi.org/10.1523/JNEUROSCI.0392-21.2021

Copyright © 2021 the authors

reaction time, fixation, and information sampling remain implicit assumptions of such frameworks. This is because in these decision-making experiments, all information is typically presented immediately and simultaneously to the participants, rather than allowing them to decide whether more information is needed.

Indeed, most studies of the neural basis of economic choice have not placed information sampling under the participant's control (Gottlieb and Oudeyer, 2018). Although neural mechanisms supporting attention (Thompson and Bichot, 2005; Bisley and Goldberg, 2010) and information sampling (Blanchard et al., 2015; Horan et al., 2019; White et al., 2019) are increasingly understood, much less is known about how future economic choices are guided by it. On the other hand, several studies have used neural implementations of evidence accumulation models to identify brain networks that show similar trial-by-trial changes in aggregate activity as the model. A region of the medial frontal cortex (MFC) that encompasses the dorsal anterior cingulate cortex (dACC) and the presupplementary motor area has been identified as correlating with accumulator activity (Venkatraman et al., 2009; Hare et al., 2011; Gluth et al., 2012; Zhang et al., 2012; Rodriguez et al., 2015; Pisauro et al., 2017). Typically, accumulator activity is greatest on trials where choice difficulty (i.e., the value of the unchosen option minus that of the chosen option) is highest, and choice difficulty itself has also previously been associated with activity in the MFC BOLD fMRI signal (Grinband et al., 2006; Pochon et al., 2008; Fitzgerald et al., 2009; Wunderlich et al., 2009; Klein-Flugge et al., 2016; Pisauro et al., 2017). It is possible, however, that accumulator fluctuations may also reflect greater information sampling on these trials. Because none of these studies explicitly measured information sampling, it is unclear which of these two accounts—choice difficulty or information sampling—better explains BOLD responses in these areas (although, importantly, they are not mutually exclusive).

Here, we used BOLD fMRI to investigate the neural basis of information sampling in economic choice by allowing participants to actively sample information in a multistep decision task. Our experimental paradigm mirrors equivalent recent paradigms used in nonhuman primates (Hunt et al., 2018) and a large-scale human behavioral study (Hunt et al., 2016). As expected from our recent work, subjects sampled more information when decisions were more difficult. When participants were first able to make a choice, fMRI signals within MFC correlated with the difficulty of the decision. Crucially, this effect was significantly reduced by including a coregressor indicating whether the subject sampled further information before choice. Activity in MFC (and bilateral intraparietal sulcus) was instead explained by the decision to sample further information.

Materials and Methods

Thirty healthy human participants (age, 18–50 years, sex not recorded) attended two study sessions: one behavioral training session (1 h) and one fMRI session (2 h 15 min). One participant was excluded from the representational similarity analyses because the person's fMRI study session was ended prematurely, meaning we did not obtain enough data from this participant to appropriately balance across different conditions. In the behavioral session, participants learned the meanings of 10 stimuli: five faces and five houses. Five of these stimuli represented a reward probability (10, 30, 50, 70, or 90%) and the other five a reward magnitude (10, 30, 50, 70, or 90 points). We ensured that whether the cues were faces or houses was orthogonal to cue values by pseudorandomizing the meaning of each cue for each participant. Specifically, there were always three face probability cues and two house probability cues (and similarly for magnitude), or vice versa, and these were interspersed so that faces or houses could not be associated with a generally low or high value (Fig. 1*B*). After learning the cues, participants were trained on the main task.

Experimental design and statistical analyses. In the main task, participants were asked to choose between two pairs of cues (Fig. 1*A*). Each pair consisted of a probability and a magnitude cue. The reward associated with that option was the number of points represented by the magnitude cue awarded probabilistically in accordance with the probability cue. Optimal behavior in the task (maximizing long-run expected reward) would be to choose the side with the higher expected value (reward probability multiplied by reward magnitude). However, a trial started with the four cues being hidden (presented as gray squares), with the pair of cues on the left as one option and the pair on the right another. Participants were initially shown two different cues sequentially, the selection of which was predetermined by the experimenter to balance cue presentation for representational similarity analyses. These could either be two cues from the same option (option trials, 50% of trials) or two cues from different options representing the same attribute (probability or magnitude; attribute trials, 50% of trials). Note that the location of each attribute was counterbalanced to be the top or bottom cue, but this was consistent between the two options within a trial (e.g., if the top cue of the left option was the probability cue, the top cue of the right option was also the probability cue). The location and identity of the first cue were counterbalanced throughout each block. The reason the cues were shown sequentially is because this enabled us to study brain activity in response to each cue separately. At the second cue, we can also study choice difficulty and belief confirmation by looking at how the neural response depends on the value difference between the options and on how well the evidence provided by the second cue conforms to that provided by the first cue. Each cue presentation lasted 2 s and was followed by a 0–4 s jittered interval during which all the cues were hidden again.

After this, participants were given the opportunity to view the remaining two hidden cues by pressing the corresponding buttons. However, participants had to pay points to do this: three points to see a third cue, and another six points to see the fourth and final cue. As such, participants had to judge how useful the additional information provided by the last two hidden cues might be in ensuring they choose the option with the highest expected value. In a pilot study, it was found that these costs typically led participants to sample further information on a subset of trials (Fig. 1*C*,*D*; although we note that the propensity to sample further information still varied across individuals). Note that participants could not choose to see the first two cues again. When participants finished sampling the additional cues, or decided they did not want to sample further cues at all, they made a choice between the two options. On half of all trials, subjects received feedback on how many points they earned that trial; feedback was only revealed on 50% of trials as this made sure stimulus-locked value-related signals and feedback-locked reward-related signals were decorrelated in the design matrix. Intertrial intervals were jittered and were between 3 and 7 s. Participants were only invited to take part in the fMRI part of the experiment if they chose the highest valued option on 70% of trials in the last practice block of the main task.

In the fMRI session, participants first received further training on the task by doing two blocks of 40 trials each outside the scanner. Inside the scanner, participants did 10 practice trials and five blocks of the main task (a total of 200 trials). Participants received £1 for every 300 points earned in the task in addition to a £20 show-up fee for coming to both study sessions. A counter in the right bottom corner of the screen kept track of the money earned up to that point throughout the task. Thus, participants earned an average of £41 overall. This experiment was realized using Cogent 2000 developed by the Cogent 2000 team at the Functional Imaging Laboratory (FIL) and the Institute of Cognitive Neuroscience (ICN) and Cogent Graphics developed by John Romaya at the Laboratory of Neurobiology (LON) at the Wellcome Department of Imaging Neuroscience.

fMRI data collection. Whole-brain fMRI measurements were made using a Siemens Prisma 3T scanner with a 2 × 2 × 2 mm voxel size, repetition time (TR) = 1.235 s, echo time (TE) = 20 ms, flip angle = 65° with an axial orientation angled to anterior commissure–posterior

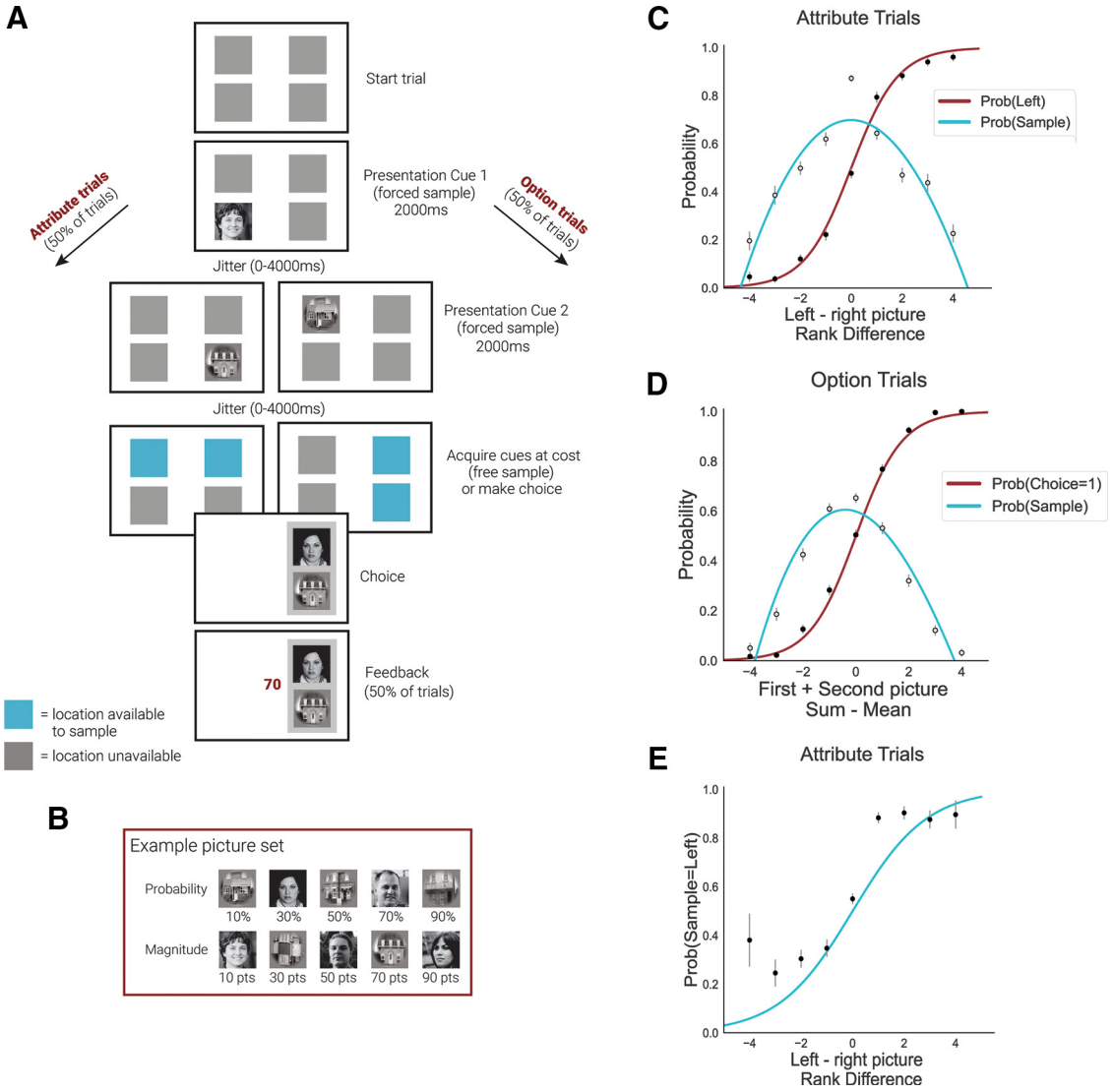

Figure 1. Experimental paradigm and participant behavior. ***A***, Task structure. The task starts with all four cues being hidden. Two cues are shown sequentially. After this, participants can choose to sample more cues or make a choice between the two options. ***B***, Example picture set and associated magnitude and probability amounts. ***A***, ***B***, Note that the pictures of faces do not belong to real individuals; they were generated. ***C***, ***D***, Participants effectively use the cue values to make correct choices and as a guide on whether more cues need to be sampled. ***C***, In attribute trials, participants are more likely to choose the left option; the larger the value difference is between the left and right observed cues. Participants are more likely to sample additional cues the closer this value difference is to zero. These psychometric curves plot the probability of choosing the left option and sampling a third cue as a function of the difference in value rank between the two revealed cues. ***D***, In option trials, participants are more likely to choose the option in which the cues have been revealed, the higher the sum of these presented cue values is compared with the mean value of an option. Participants are more likely to sample additional cues the closer this value sum is to the mean. ***C***, ***D***, Psychometric curves plot the probability of choosing the option in which the cues were revealed and sampling a third cue as a function of the sum of the ranked values of the revealed cues subtracting the mean cue rank of an option. ***E***, Participants were more likely to sample the remaining hidden cue from the option with the highest revealed cue value in attribute trials. This psychometric curve plots the probability of sampling cues from the left option as a function of the difference in value rank between the two revealed cues and only plots trials in which participants sampled additional cues. ***C***,***D***,***E***: error bars reflect the standard error of the mean.

commissure using a 64-channel head coil. The sequence used was MB3 PAT2. Participants performed five blocks of the main task inside the scanner with short breaks in between. For each new block a new run was initiated. Given that the task was not speeded, the runs were of variable length as were the number of volumes collected per run. The average number of volumes collected per participant was 2587. T1-weighted structural images were obtained using an MPRAGE sequence with 1 × 1 × 1 mm voxel size, on a 174 × 192 × 192 grid, TE = 3.97 ms, TR = 1.9 s. A field map with dual echo-time images was also acquired (TE = 7.38 ms, whole-brain coverage, 2.4 × 2.4 × 2.4 mm voxel size).

fMRI data analysis. fMRI analysis was conducted using the Centre for Functional MRI of the Brain (FMRIB) Software Library (FSL), and custom-written representational similarity analysis (RSA) scripts in MATLAB, which built on the Representational Similarity Analysis toolbox (Nili et al., 2014).

The preprocessing performed on the data were the following: motion correction using MCFLIRT (FMRIB Linear Image Registration Tool with motion correction; Jenkinson et al., 2002), nonbrain removal using BET (Brain Extraction Tool; Smith, 2002), spatial smoothing using a Gaussian kernel of FWHM 5 mm; grand-mean intensity normalization of the entire 4D dataset by a single multiplicative factor, and highpass temporal filtering (Gaussian-weighted least-squares straight line fitting, with σ = 50.0 s). Registration to high resolution structural and/or standard space images was conducted using FLIRT (FMRIB Linear Image Registration Tool; Jenkinson and Smith, 2001; Jenkinson et al., 2002).

Behavioral data analysis. We studied the effects of cue value on choice and sampling decisions using single-subject logistic regressions followed by one-sample *t* tests on the single-subject regression coefficients (Fig. 1*C*,*D*). Specifically, we performed two logistic regressions on

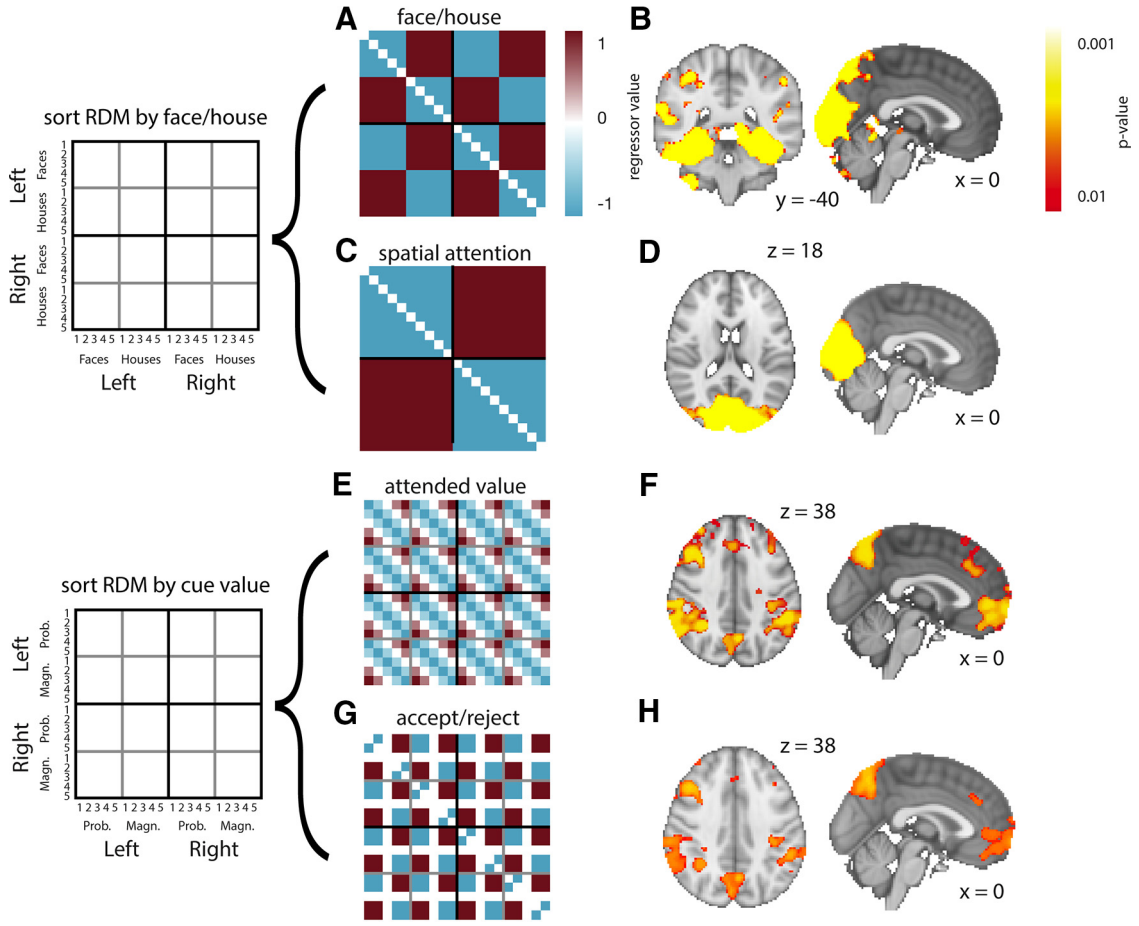

Figure 2. ***A***, ***C***, ***E***, ***G***, Whole-brain searchlight analysis reveals representations of several features of the task. RSA templates for spatial attention, face/house category, attended value, and accept/reject. ***B***, Cue category (face or house) is represented in the visual and inferior temporal cortex. ***D***, Spatial attention is represented in the visual cortex. ***E–H***, We find activations for attended value and accept/reject in an elaborate network including the vmPFC, ACC, and the posterior parietal cortex. All parametric maps depict *p* values derived from using TFCE on GLM *z*-score maps.

attribute trials where the independent variable was the value rank difference between the left and right presented cues, and the dependent variable was whether the left option was chosen or whether a third cue was sampled, respectively. Similarly, on option trials two logistic regressions were executed where the independent variable was the summed cue ranks of the two presented cues minus the mean value rank of an option, and the dependent variable was whether the fully revealed option was chosen or whether a third cue was sampled, respectively.

RSA. We first estimated a whole-brain general linear model (GLM) with regressors encoding onsets of the first two cues, cue category (face or house), and which side of the screen the cue appeared on. This GLM was executed on the spatially smoothed data. Then, we performed searchlight RSA, meaning RSA is performed for a 100-voxel sphere of voxels, centered around each voxel in the brain (Nili et al., 2014). These were then regressed against model representational similarity matrices (Fig. 2) to find areas of the brain where activity showed similar representations. We then performed a statistical test at each voxel, and significant clusters were identified using threshold-free cluster enhancement (TFCE; Smith and Nichols, 2009). The resulting *p* values were familywise error (FWE) rate controlled at a threshold of $p < 0.05$. This same method was used with representational similarity matrices obtained from Hunt et al. (2018) to investigate similarities between representations in the monkey and the human prefrontal cortex, although here we present unthresholded statistical maps as no clusters survived multiple comparisons correction in PFC.

Mass univariate analysis. Two GLMs were fit to the individual subject data, one including and one excluding regressors describing information sampling behavior. We also included regressors describing the onset of the first two cues, cue values (separated into cues where the associated option was eventually chosen or unchosen), the side of cue presentation, trial type (option or attribute trial), and whether feedback was presented, and if so, how much reward the participant received on the preceding trial. Finally, our model included a regressor that reflected belief confirmation, encoded as an index defining how much the second cue should change the agent's belief about what the best option is (see Fig. 5). We used contrasts of parameter estimates to find regions that encoded the inverse value difference between the revealed cues (i.e., unchosen minus chosen value, or choice difficulty). All regressors were modeled as 2 s boxcar functions to match the duration that the cue was presented. We report mass univariate results at the group level using whole-brain FWE-corrected statistical significance and a cluster significance threshold of $z > 2.3$ and $p < 0.05$. Note that similar results were obtained using TFCE (Smith and Nichols, 2009).

To measure how much the main effect of choice difficulty was reduced by adding the information sampling regressor (see Fig. 4), without being biased by the initial GLM, we used a leave-one-out procedure. BOLD activity was extracted for each participant from the choice difficulty (in both GLMs) and information sampling contrasts using a region of interest (ROI) defined by a group model excluding that participant. The ROI was defined as any positively significant clusters ($z > 3.1$, $p < 0.05$, corrected) for the contrast of inverse value difference found within a large mediofrontal mask. We then performed a one-sample *t* test on the extracted parameter estimates for the inverse value difference contrast, both including or excluding information sampling behavior as a coregressor.

Data availability. Unthresholded *z* statistic maps for all analyses are available at https://neurovault.org/collections/9314/. Code for the task,

behavioral data, and all behavioral analyses can be found at https://git.fmrib.ox.ac.uk/comp-cog-neuro/behavioral-data-and-analyses-from-kaanders-2021.git. The RSA results were produced using the RSA toolbox from the Medical Research Council Cognition and Brain Sciences Unit, University of Cambridge, at https://www.mrc-cbu.cam.ac.uk/methods-and-resources/toolboxes/.

Results

Thirty healthy human participants (age, 18–50 years) performed an information-gathering and economic choice task inside the MRI scanner (Fig. 1*A*). In the task, they were asked to choose between two pairs of cues, where the pair of cues on the left were one choice option and the pair on the right another. Each pair consisted of a probability and a magnitude cue. The reward associated with an option was the number of points represented by the magnitude cue awarded probabilistically in accordance with the probability cue. The cues were pictures of faces and houses, and the magnitude or probability associated with them was learned by the participants in a behavioral session that took place before the main experiment (Fig. 1*B*). Optimal behavior in the task (maximizing the long-run expected reward) would be to choose the option with the higher expected value (= reward probability * magnitude).

Crucially, each trial started with the four cues being hidden. Participants were initially shown two of the hidden cues sequentially in a pseudorandom order determined by the experimenter. These could either be two cues from the same option (option trials, 50% of trials) or two cues from different options representing the same attribute (probability or magnitude; attribute trials, 50% of trials). After these first two cues had been viewed, participants could choose whether to sample the remaining hidden cues by pressing the corresponding buttons and paying a small number of points (−3 points to sample the third cue, −6 points to sample the fourth cue). Alternatively, participants could forgo the opportunity to sample further information and instead make a choice between the two options based on the information sampled thus far. Subjects then received feedback on how many points they earned that trial, although to decouple this hemodynamic response from that of the decision onset, feedback was only delivered on half of all trials (Guitart-Masip et al., 2011).

Both participants' eventual choices, and their propensity to sample more information before choice, depended on the values associated with the first two presented cues. In attribute trials, their choices were a function of the difference in value between the left and right cues ($t_{(29)} = 10.79$, $p < 0.001$; Fig. 1*C*), whereas in option trials their choices depended on the value of the option relative to the mean expected value ($t_{(29)} = 15.88$, $p < 0.001$; Fig. 1*D*). Importantly, participants' decision to sample a third piece of information also depended on these cue values, so the more difficult the decision, the more information was sampled ($t_{(29)} = -2.11$, $p = 0.04$ on attribute trials; $t_{(29)} = -7.20$, $p < 0.001$ on option trials; Fig. 1*C*,*D*). In attribute trials, the direction of this sample tended to be biased toward the option that currently had the highest value (Fig. 1*E*), a bias also observed in our previous monkey (Hunt et al., 2018) and large-scale human behavioral studies (Hunt et al., 2016).

We first performed a whole-brain searchlight RSA, using templates representing several features of the task at the time of presentation of the first cue (Fig. 2). At each 100-voxel searchlight sphere, we regressed the templates onto the RSA matrix of that location to find the regions where brain activity showed a similar representation. Several of these templates were the same as those used in our previous study using single-unit recording in macaques (Hunt et al., 2018). First, as a positive control for the success of our searchlight RSA pipeline, we included a face/house template that represented which category a cue belonged to (Fig. 2*A*). Replicating numerous RSA results in the prior literature (Kriegeskorte et al., 2008; Dima et al., 2018), this produced a strong correlation with the visual and inferior temporal cortex [peak Montreal Neurological Institute (MNI) coordinates at (31, −61, −9) and peak $z = 12.37$, $p < 0.001$, Fig. 2*C*]. Consistent with previous studies, these results were robust and replicable even at the level of individual participants. The next template identified regions where the multivariate activity distinguished between whether the currently presented cue was on the left or right hand side of the screen (Fig. 2*C*). As expected, this was strongly represented in the primary visual cortex [peak MNI coordinates at (−6, −85, 4) and peak z = 11.28, $p < 0.001$, Fig. 2*D*]. Surprisingly, however, we did not find activation in frontal eye fields or the dorsolateral prefrontal cortex, despite this pattern clearly being represented in the dorsolateral prefrontal cortex (dlPFC) in our previous single-unit data (Hunt et al., 2018).

To investigate the neural correlates of the value-related features of the task, we included attended value and accept/reject templates, mirroring those in our previous study (Hunt et al., 2018). The attended value template simply represents the value of the first cue, ranked from 1 to 5 and then normalized so that low-value cues are predicted to be similar to other low-value cues, and high-value cues are predicted be similar to other high-value cues (Fig. 2*E*). The template assumes that magnitude and probability cues were treated the same in terms of how valuable they were because to calculate the expected value of an option participants had to collapse across the two cues and because magnitude and probability cues were found to be similarly encoded in the macaque orbitofrontal cortex (OFC) single-cell recordings (Hunt et al., 2018). The accept/reject template also represents the value of the first cue but binarizes this into above average or below average in value (or neutral, for the midvalue cue; Fig. 2*G*). In our single-unit data, this correlated with activity in the dACC (Hunt et al., 2018). In our fMRI data, we found that both the attended value and accept/reject templates correlated with the activity in an extensive network within the frontal and parietal cortices, including the ventromedial PFC [vmPFC; peak at MNI coordinates (2, 50, −1) and peak $z = 4.36$, $p < 0.001$ for attended value template; peak at MNI coordinates (2, 51, 1) and peak $z = 3.90$, $p = 0.006$ for accept/reject template], dACC [peak at MNI coordinates (0, 37, 29) and peak $z = 4.80$, $p = 0.003$ for attended value template; peak at MNI coordinates (0, 35, 31) and peak $z = 5.91$, $p = 0.006$ for accept/reject template], and the posterior parietal cortex [peak at MNI coordinates (52,−49, 51) and peak $z = 5.91$, $p < 0.001$ for attended value template; peak at MNI coordinates (52, −49, 51) and peak $z = 5.14$, $p = 0.002$ for accept/reject template; Fig. 2*E*–*H*]. As expected, this network corresponds well with areas previously identified in meta-analyses of subjective value encoding using fMRI (Bartra et al., 2013; Clithero and Rangel, 2014).

We then investigated the neural correlates of the decision to sample further information, which first occurred at the time of presentation of the second cue, and whether this might explain activations that would otherwise be described as encoding choice difficulty. To test this, we used a mass univariate analysis as the task comprised too many conditions to perform RSA at the time of presentation of the second cue. In an initial analysis, we included only the values of the different cues as regressors and found a subregion of MFC that was negatively related to the difference between the values of the chosen and unchosen options,

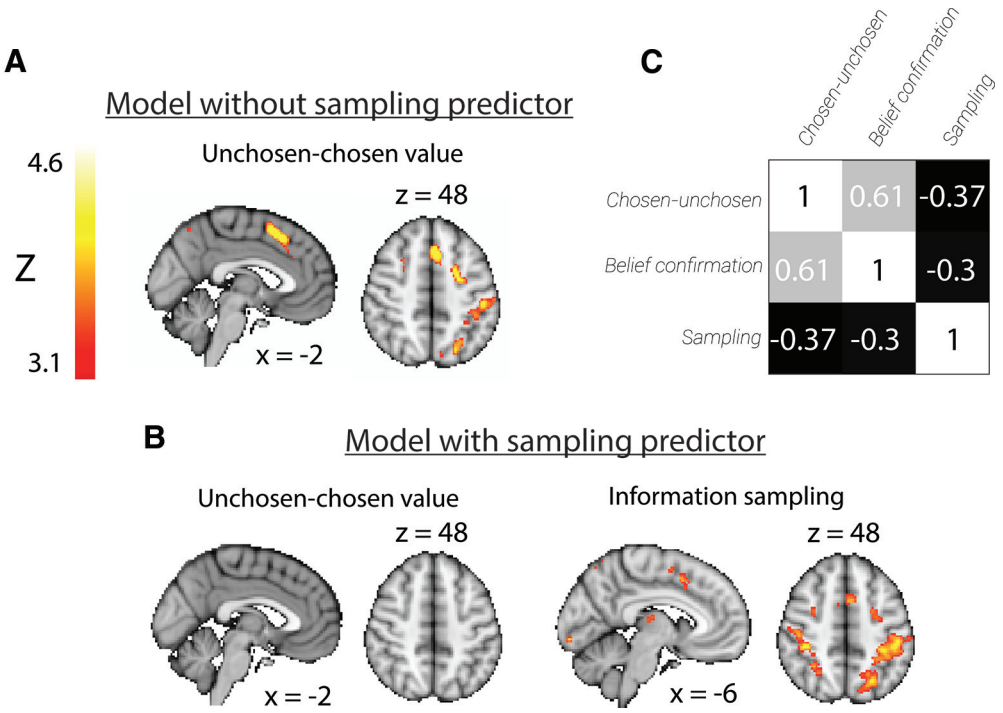

Figure 3. There is a main effect of inverse value difference (choice difficulty) at the time of presentation of cue 2 in MFC, which disappears when subsequent information sampling is included as a regressor. ***A***, Linear positive effect of inverse value difference in MFC in 30 subjects. ***B***, There is no effect of inverse value difference in MFC when information sampling is included as a regressor, although there is a linear positive effect of information sampling in MFC in 24 subjects. All parametric maps are cluster corrected and thresholded at $z > 3.1$. ***C***, Correlation matrix of value difference, belief confirmation, and sampling predictors in mass univariate analysis in 24 subjects.

which we refer to as "inverse value difference" [Fig. 3*A*, peak at MNI coordinates (−4, 15, 50) and peak $z = 6.27$]. In other words, activity in this region was greater for more difficult decisions, replicating a large number of previous findings in the economic choice literature (Grinband et al., 2006; Pochon et al., 2008). Low-level sensory features were counterbalanced across value levels (Fig. 1*B*) and across participants, so this effect was only because of the value difference between the choice options. In option trials, the choice difficulty was defined as the value difference between the revealed option and the mean expected value of a choice option. In attribute trials, choice difficulty was defined as the value difference between the revealed cues. A main effect of choice difficulty was seen looking across all trials, and when splitting by trial type the effect was also present both on option trials and attribute trials.

Crucially, this model did not yet account for whether participants chose to sample further information before committing to one of the options. In a further regression model, we included a binary information sampling regressor describing whether participants chose to sample more information on a given trial. As expected from the relationship between difficulty and information sampling (Fig. 1*C*,*D*), this regressor had some correlation with the regressor encoding value difference (average correlation of $r = -0.3$; Fig. 3*C*; we note that six participants were excluded from this analysis as they sampled additional information before choosing less than once per block). We found that the main effect of choice difficulty in MFC disappeared when the information sampling predictor was included, and this was not a consequence of the exclusion of the six participants who rarely sampled further information. Instead, a main effect of information sampling was seen in a small section of MFC, which was more active on trials where subjects decided to sample further information [Figs. 3*B*, 4, peak activation at MNI coordinates (−6, 10, 46) and peak $z = 4.04$]. We also tested whether any other regions encoded choice difficulty after inclusion of the regressor that reflects information sampling; no regions were found to survive correction for multiple comparisons, although some subthreshold activations remained (unthresholded statistical maps, both including and excluding information sampling coregressors, are available at https://neurovault.org/collections/9314/). It is important to note that this effect cannot be attributed to variations in response times, and thus trial durations, as participants were only allowed to respond after viewing the second cue for 2 s and a 0–4 s jitter. All regressors in this analysis were modeled as 2 s boxcar functions to reflect the duration of cue presentations. Consistent with recent reports that highlight the role of the parietal cortex in reducing uncertainty about future rewards (Horan et al., 2019), we also found bilateral activation of the intraparietal sulcus for this regressor [peak activation at MNI coordinates (−36, −32, 42) and peak $z = 5.78$; Fig. 3*B*).

To further explore whether choice difficulty encoding was significantly reduced by the inclusion of the information sampling regressor, we performed a region-of-interest analysis. We focused our results on the MFC region that encoded inverse value difference (i.e., choice difficulty) in the whole-brain analysis (Fig. 3*A*), but to avoid circularity (Kriegeskorte et al., 2009), we used a leave-one-out procedure in which each participant's ROI was defined by taking significant MFC voxels from a group model including all participants except them (Boorman et al., 2013). This revealed a significant reduction in the encoding of inverse value difference as a consequence of including the information sampling regressor (Fig. 4*B*; $t_{(23)} = 3.28$, $p = 0.003$) so that choice difficulty was no longer significantly encoded in this region ($t_{(23)} = 1.17$, $p = 0.26$). Instead, this region of interest significantly encoded the decision to sample further information (Fig. 4*C*; $t_{(23)} = 4.17$, $p < 0.001$).

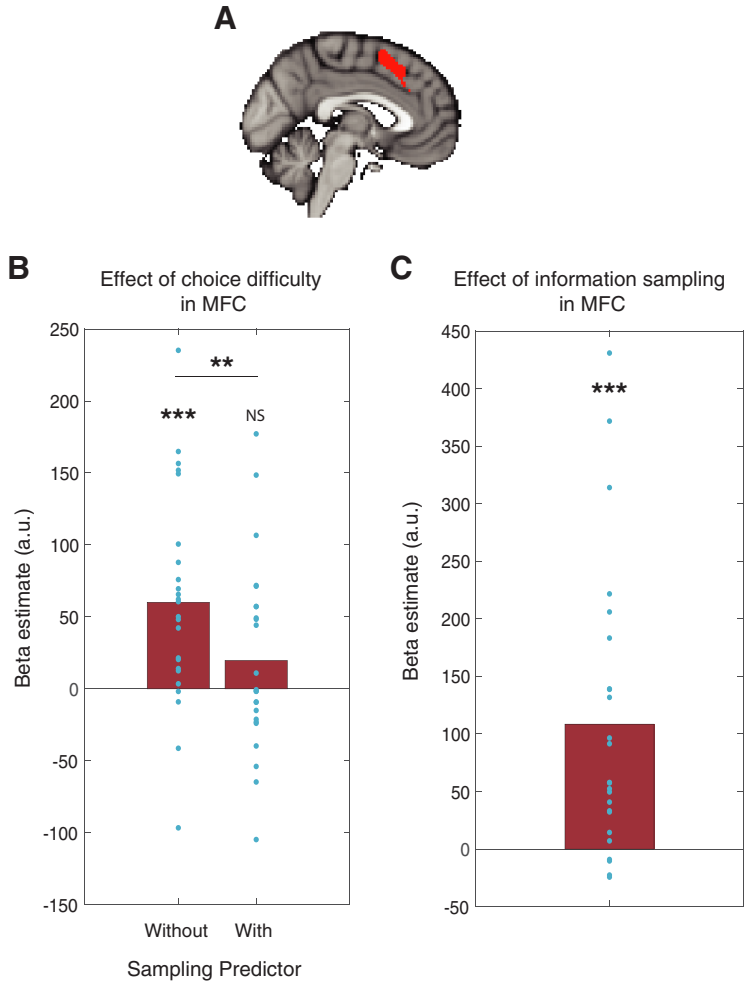

Figure 4. When information sampling is included as a coregressor there is a significant decrease in the main effect of inverse value difference (in an MFC region of interest equivalent to the region defined in Fig. 3*A*, a leave-one-out procedure). ***A***, MFC region of interest derived from mass univariate analysis including all 30 subjects, focusing on the region that maximally encodes choice difficulty. ***B***, Effect of inverse value difference in MFC in GLMs with and without the information sampling coregressor in 24 subjects. ***C***, Effect of information sampling in the same brain region. A stronger BOLD signal was found in this region on trials where participants would subsequently decide to sample more information before committing to a choice compared with trials where they made a choice straightaway. ***B***, ***C***: NS: not significant, **: $p < 0.01$, ***: $p < 0.001$.

We also investigated encoding of belief confirmation, which was defined as the extent to which the value of the second cue confirmed the belief formed after presentation of the first cue. In our single-unit study, we found that belief confirmation was reliably encoded in dACC (Hunt et al., 2018), and similarly in the present study, we found fMRI activity in a more anterior portion of MFC-encoded belief confirmation on option trials [Fig. 5*A*; peak $z = 4.81$ at peak at MNI coordinates (8, 34, 8)). However, this effect did not survive whole-brain correction in the reduced sample of the 24 participants who regularly sampled more information before choosing. We again used a leave-one-out procedure to determine how this effect changed as a result of reducing the sample size and including the information sampling regressor (Fig. 5*C*). Although there is only a significant main effect of belief confirmation in MFC in the large sample of 30 participants ($t_{(28)} = 2.54$, one-tailed $p = 0.008$), this effect is not significantly reduced by excluding participants and including the sampling predictor from the model ($t_{(51)} = 0.06$, $p = 0.952$; $t_{(23)} = -0.002$, $p = 0.998$).

Finally, we hypothesized RSA could also be a way of identifying functional homologues of macaque prefrontal subregions in the human brain. To study task representations across species, we used the RSA matrices found in single-cell recordings in three prefrontal regions in the macaque (Hunt et al., 2018) for another whole-brain searchlight RSA (Fig. 6). Prefrontal BOLD activity from the human brain was not found to be significantly correlated with any of these macaque RSA matrices. However, some subthreshold activations of interest were found. The macaque ACC matrix was correlated with human anterior insula activity [peak at MNI coordinates (−28, 24, −3) and peak $z = 3.97$] and the macaque OFC matrix was correlated with human vmPFC activity [peak at MNI coordinates (0, 46, 9) and peak $z = 3.34$]. A strong correlation was found between the macaque dlPFC matrix and human visual cortex, which was expected as the macaque dlPFC strongly represented spatial attention on this task [peak at MNI coordinates (−5, −88, 3) and peak $z = 21.16$].

Discussion

Here, we have shown that in an information sampling and economic choice task, MFC activity encodes whether a subject will sample further information before committing to a decision. Moreover, we found that this effect could explain away the encoding of choice difficulty (inverse value difference) in MFC, a signal that has been commonly observed in many previous studies of economic choice (Grinband et al., 2006; Pochon et al., 2008). Our findings should not be interpreted as suggesting that difficulty is not encoded in MFC, but instead that difficulty is a fundamental determinant of whether further information is sampled before choice. Here, we have defined choice difficulty purely in terms of the complexity of the value comparison between two choice options. As the low-level sensory features of the cues are similar across the different cues, value comparison is the only source of choice difficulty in this task. However, difficulty is not necessarily identical to choice uncertainty. In fact, trial-to-trial changes in decision confidence can in certain circumstances be dissociated from choice difficulty (De Martino et al., 2013); it is possible that such metacognitive fluctuations may be linked to or even predictive of information sampling.

Our findings form a logical extension of previous work on the role of MFC as an evidence accumulator (Venkatraman et al., 2009; Hare et al., 2011; Gluth et al., 2012; Zhang et al., 2012; Rodriguez et al., 2015; Pisauro et al., 2017) as evidence accumulation involves an implicit decision to sample further information when a decision boundary has not yet been reached (Shadlen and Shohamy, 2016). An advantage of the current information-gathering paradigm is that it allowed us to study the relationship between MFC signals and subsequent behavior; most paradigms in the field are much simpler and do not allow for this type of analysis.

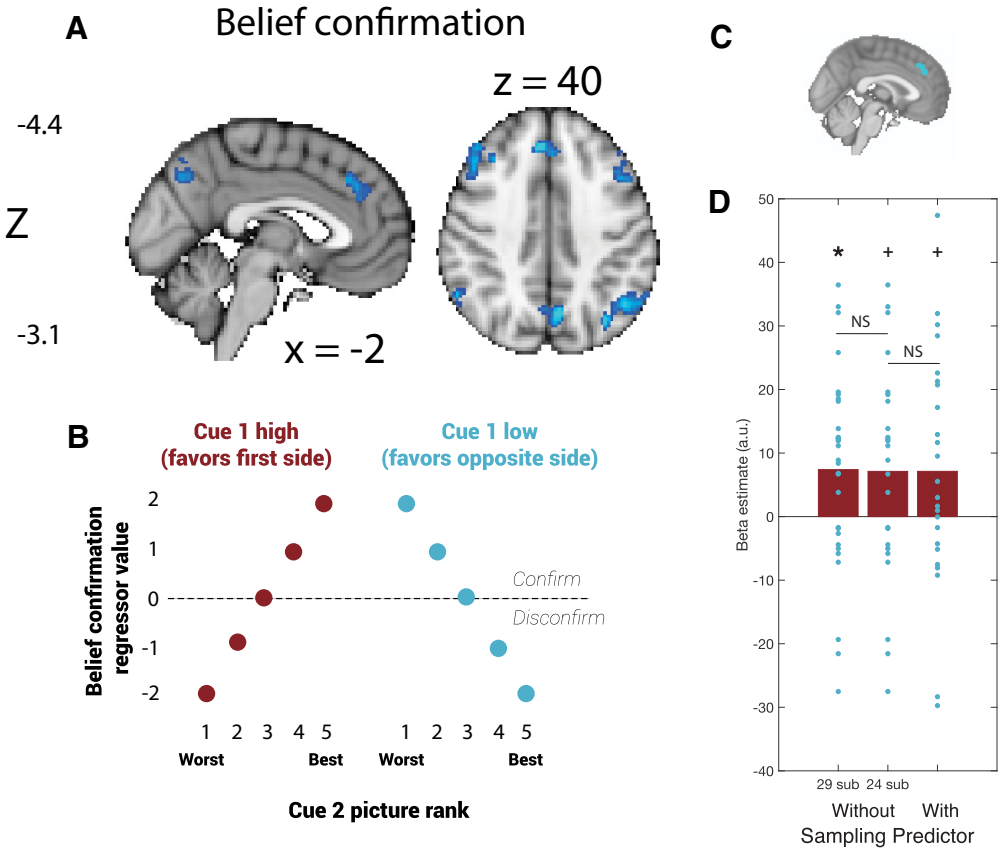

Figure 5. A main effect of belief confirmation was also found in MFC on option trials, but this effect disappeared when using the reduced sample of 24 subjects. ***A***, Linear negative effect of belief confirmation in MFC on option trials in 30 subjects. Parametric maps are cluster corrected and thresholded at $z < -3.1$. ***B***, Encoding of belief confirmation as a function of the ranks of the two presented cues. ***C***, MFC region of interest derived from mass univariate analysis including all 30 subjects. ***D***, Effect of belief confirmation in option trials in MFC in GLMs with 29 subjects or 24 subjects and with and without the sampling predictor. ***D***: NS: not significant, +: one-tailed $p < 0.05$, *: $p < 0.05$.

Our findings are consistent with previous studies that propose a role for MFC in guiding exploratory behavior (Daw et al., 2006; Boorman et al., 2009; Hayden et al., 2009; Badre et al., 2012; Kolling et al., 2012; Domenech et al., 2020). For example, a study by Blanchard and Gershman (2018) contrasted trials in which participants decided to place a bet versus trials where they decided to obtain further information about the value of that bet. Activity in MFC and bilateral insula was significantly greater on observe trials than on bet trials (we also found subthreshold activity in the insula predictive of information sampling; maps at https://neurovault.org/collections/9314/). Similarly, a single-unit recording study by White et al. (2019) identified dACC as the leading node in a network of areas that encoded gaze shifts to resolve uncertainty about upcoming rewards, and further studies have shown that activity in this area predicts checking behaviors when monkeys are close to receiving a reward (Stoll et al., 2016). Collectively, this work is consistent with a role for this region in driving information sampling to resolve uncertainty (Monosov, 2020), which in turn gives rise to shifts in visual fixation and spatial attention (Krauzlis et al., 2014; Gottlieb et al., 2020).

More broadly, different subregions of MFC have been associated with diverse parameters in different paradigms (Kolling et al., 2016), whether it is sampling value (Stoll et al., 2016), conflict (Botvinick et al., 1999), choice difficulty (Grinband et al., 2006; Pochon et al., 2008), or belief disconfirmation/confirmation (Quilodran et al., 2008; Wessel et al., 2012; Boorman et al., 2013; Hunt et al., 2018). It is notable that all these task parameters may affect the degree to which additional information sampling is required before committing to a choice. On the other hand, it has also been suggested that dACC is particularly active when participants switch from a default behavior (Boorman et al., 2013; Kolling et al., 2016). It is possible that we find mediofrontal activity predictive of information sampling because in our study not sampling additional information could be considered a default behavior, given that participants commit to a choice straightaway more often than they decide to sample more cues (Fig. 1*C*,*D*).

Our behavioral results also indicate that humans are more likely to sample information from an option they believe is good (Fig. 1*E*), consistent with our previous behavioral findings (Hunt et al., 2016). We hypothesize that MFC may therefore drive information sampling through active hypothesis testing (Markant and Gureckis, 2012). This is consistent with the presence of a belief confirmation signal in ACC, which we find here (Fig. 5) and also in our previous single-unit study (Hunt et al., 2018). This effect was not reduced by including an information sampling predictor. It is also consistent with recent behavioral findings in perceptual decision-making (Talluri et al., 2018), and the recent suggestion that gaze affects the integration of goal-relevant evidence rather than value in economic choice (Sepulveda et al., 2020). Such an account of economic choice has recently been proposed as particularly ecologically valid in decisions containing multiple options (Hayden, 2018). More detailed testing of this hypothesis will require paradigms in which multiple options are available for choice, and where information sampling and choice are explicitly dissociated from one another.

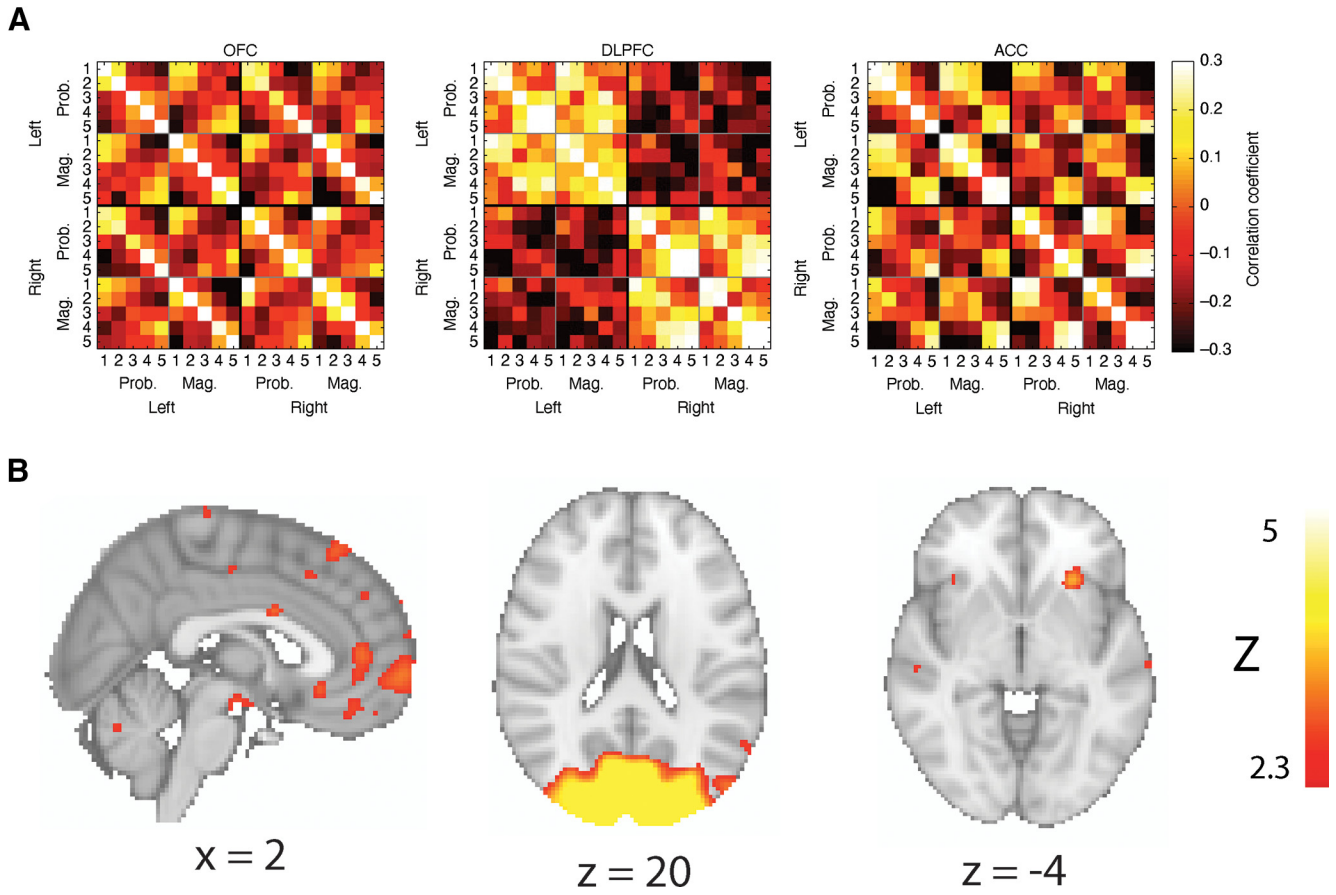

Figure 6. ***A***, To further investigate RSA as a method to link functional data across species (Kriegeskorte et al., 2008), we performed a whole-brain searchlight on the human fMRI data using RSA matrices derived directly from the single-unit recordings measured in three relevant prefrontal regions in macaques, instead of using model RSA matrices as in Figure 2 (Hunt et al., 2018). ***B***, No significant whole-brain cluster-corrected correlations were found within the human prefrontal cortex, although subthreshold activations were found in human insula correlated with the macaque ACC matrix and the human vmPFC correlated with the macaque OFC matrix. As expected from the result in Figure 2, *C* and *D*, the human visual cortex was found to be related to the macaque dlPFC matrix, which strongly reflected the participant's current locus of spatial attention. All parametric maps are uncorrected and thresholded at $z > 2.3$.

We were able to identify brain networks encoding both sensory- and value-related aspects of the task using RSA, some of which encompassed areas in PFC (Fig. 2), where value responses have previously been shown using multivariate pattern analysis (Kahnt et al., 2010). A similar region was found to encode continuous and categorial (below or above average) attended value. We tested for the presence of these two regressors despite their correlation because in the macaque single-cell data from Hunt et al., (2018), continuous value was found to be mostly encoded in OFC, whereas categorical value was encoded in ACC. In the same analysis, we also observed value-related activity in the bilateral parietal cortex, which is consistent with a similar RSA regressor used to describe parietal cortex EEG responses to numerical magnitude in an economic choice task (Luyckx et al., 2019).

The clear correlation between templates describing the visual properties of cues in the task and visual/inferotemporal cortical activity replicates earlier work showing that RSA distinguishes objects of different categories in these areas in human fMRI data (O'Toole et al., 2005; Kriegeskorte et al., 2008; Dima et al., 2018). It has previously been suggested that such an approach can be used to study representations across species, found using different types of data (Kriegeskorte et al., 2008). We hypothesized that our task might allow us to perform a similar cross-species analysis to identify functional homologues of the PFC subregions studied with single-unit recordings in Hunt et al., (2018). We did not clearly identify the same triple dissociation that was seen in our previous study (Fig. 6).

It is possible that we were not sensitive to detect a dissociation in PFC here similar to that in Hunt et al. (2018) because of the lower signal-to-noise ratio in human fMRI data compared with that in single-cell data. It still remains unclear whether RSA really probes fine-grained spatial information that is similar to that identified by single neuron data, or whether it is primarily driven by the same macroscopic signals that can also be isolated in mass univariate analyses (Op de Beeck, 2010). It is possible that the intermixed positive and negative coding that supported the successful RSA in Hunt et al. (2018) is not observable at the voxel level in a human fMRI. This may also explain why decoding accuracies in multivariate pattern analyses are invariably far lower in the prefrontal cortex than in the occipital and temporal cortices (Bhandari et al., 2018). It is also clear there are differences in the nature of the spiking and BOLD signal, which mean that certain features that are readily decodable in single-unit data cannot be found using an equivalent analysis of fMRI data (Dubois et al., 2015). In addition to this, despite the similarity between the present task and our previous monkey study, there are also some obvious differences. For example, monkeys were trained on the task for several months beforehand (Hunt et al., 2018) whereas humans were only trained shortly before entering the scanner. Although both performed the task well with similar patterns of behavior, they may have approached the task using

different strategies. It is also possible that the differences could result from anatomic differences between the human and monkey PFC, yet all the regions previously studied in the macaque have direct homologues in the human (Sallet et al., 2013; Neubert et al., 2015); we therefore believe this to be an unlikely explanation for the difference.

In summary, we have shown that MFC activity in economic choice predicts subsequent information sampling. We replicated previous studies showing that MFC activity in different subregions is related to choice difficulty, but critically this effect was explained away by the inclusion of information sampling as a coregressor. This suggests that the role of MFC may extend beyond that of evidence accumulation and implies an important role for MFC in guiding adaptive information sampling during economic choice.

References

Badre D, Doll BB, Long NM, Frank MJ (2012) Rostrolateral prefrontal cortex and individual differences in uncertainty-driven exploration. Neuron 73:595–607.

Bartra O, McGuire JT, Kable JW (2013) The valuation system: a coordinate-based meta-analysis of BOLD fMRI experiments examining neural correlates of subjective value. NeuroImage 76:412–427.

Bettman JR, Luce MF, Payne JW (1998) Constructive consumer choice processes. J Consum Res 25:187–217.

Bhandari A, Gagne C, Badre D (2018) Just above chance: is it harder to decode information from prefrontal cortex hemodynamic activity patterns? J Cogn Neurosci 30:1473–1498.

Bisley JW, Goldberg ME (2010) Attention, intention, and priority in the parietal lobe. Annu Rev Neurosci 33:1–21.

Blanchard TC, Gershman SJ (2018) Pure correlates of exploration and exploitation in the human brain. Cogn Affect Behav Neurosci 18:117–126.

Blanchard TC, Hayden BY, Bromberg-Martin ES (2015) Orbitofrontal cortex uses distinct codes for different choice attributes in decisions motivated by curiosity. Neuron 85:602–614.

Boorman ED, Behrens TEJ, Woolrich MW, Rushworth MFS (2009) How green is the grass on the other side? frontopolar cortex and the evidence in favor of alternative courses of action. Neuron 62:733–743.

Boorman ED, Rushworth MF, Behrens TE (2013) Ventromedial prefrontal and anterior cingulate cortex adopt choice and default reference frames during sequential multi-alternative choice. J Neurosci 33:2242–2253.

Botvinick M, Nystrom LE, Fissell K, Carter CS, Cohen JD (1999) Conflict monitoring versus selection- for-action in anterior cingulate cortex. Nature 402:179–181.

Busemeyer JR, Townsend JT (1993) Decision field theory: a dynamic-cognitive approach to decision making in an uncertain environment. Psychol Rev 100:432–459.

Clithero JA, Rangel A (2014) Informatic parcellation of the network involved in the computation of subjective value. Soc Cogn Affect Neurosci 9:1289–1302.

Daw ND, O'Doherty JP, Dayan P, Seymour B, Dolan RJ (2006) Cortical substrates for exploratory decisions in humans. Nature 441:876–879.

De Martino B, Fleming SM, Garrett N, Dolan RJ (2013) Confidence in value-based choice. Nat Neurosci 16:105–110.

Dima DC, Perry G, Singh KD (2018) Spatial frequency supports the emergence of categorical representations in visual cortex during natural scene perception. Neuroimage 179:102–116.

Domenech P, Rheims S, Koechlin E (2020) Neural mechanisms resolving exploitation-exploration dilemmas in the medial prefrontal cortex. Science 369:eabb0184.

Dubois J, de Berker AO, Tsao DY (2015) Single-unit recordings in the macaque face patch system reveal limitations of fMRI MVPA. J Neurosci 35:2791–2802.

FitzGerald THB, Seymour B, Dolan RJ (2009) The role of human orbitofrontal cortex in value comparison for incommensurable objects. J Neurosci 29:8388–8395.

Gluth S, Rieskamp J, Büchel C (2012) Deciding when to decide: time-variant sequential sampling models explain the emergence of value-based decisions in the human brain. J Neurosci 32:10686–10698.

Gottlieb J, Oudeyer PY (2018) Towards a neuroscience of active sampling and curiosity. Nat Rev Neurosci 19:758–770.

Gottlieb J, Cohanpour M, Li Y, Singletary N, Zabeh E (2020) Curiosity, information demand and attentional priority. Curr Opin Behav Sci 35:83–91.

Grinband J, Hirsch J, Ferrera VP (2006) A neural representation of categorization uncertainty in the human brain. Neuron 49:757–763.

Guitart-Masip M, Fuentemilla L, Bach DR, Huys QJM, Dayan P, Dolan RJ, Duzel E (2011) Action dominates valence in anticipatory representations in the human striatum and dopaminergic midbrain. J Neurosci 31:7867–7875.

Hare TA, Schultz W, Camerer CF, O'Doherty JP, Rangel A (2011) Transformation of stimulus value signals into motor commands during simple choice. Proc Natl Acad Sci U S A 108:18120–18125.

Hayden BY (2018) Economic choice: the foraging perspective. Curr Opin Behav Sci 24:1–6.

Hayden BY, Pearson JM, Platt ML (2009) Fictive reward signals in the anterior cingulate cortex. Science 324:948–950.

Horan M, Daddaoua N, Gottlieb J (2019) Parietal neurons encode information sampling based on decision uncertainty. Nat Neurosci 22:1327–1335.

Hunt LT, Kolling N, Soltani A, Woolrich MW, Rushworth MFS, Behrens TEJ (2012) Mechanisms underlying cortical activity during value-guided choice. Nat Neurosci 15:470–476.

Hunt LT, Rutledge RB, Malalasekera WMN, Kennerley SW, Dolan RJ (2016) Approach-induced biases in human information sampling. PLOS Biol 14: e2000638.

Hunt LT, Malalasekera WMN, de Berker AO, Miranda B, Farmer SF, Behrens TEJ, Kennerley SW (2018) Triple dissociation of attention and decision computations across prefrontal cortex. Nat Neurosci 21:1471–1481.

Jamieson DG, Petrusic WM (1977) Preference and the time to choose. Organ Behav Hum Perform 19:56–67.

Jenkinson M, Smith S (2001) A global optimisation method for robust affine registration of brain images. Med Image Anal 5:143–156.

Jenkinson M, Bannister P, Brady M, Smith S (2002) Improved optimization for the robust and accurate linear registration and motion correction of brain images. NeuroImage 17:825–841.

Kahnt T, Heinzle J, Park SQ, Haynes J-D (2010) The neural code of reward anticipation in human orbitofrontal cortex. Proc Natl Acad Sci U S A 107:6010–6015.

Klein-Flugge MC, Kennerley SW, Friston K, Bestmann S (2016) Neural signatures of value comparison in human cingulate cortex during decisions requiring an effort-reward trade-off. J Neurosci 36:10002–10015.

Kobayashi K, Ravaioli S, Baranès A, Woodford M, Gottlieb J (2019) Diverse motives for human curiosity. Nat Hum Behav 3:587–595.

Kolling N, Behrens TEJ, Mars RB, Rushworth MFS (2012) Neural mechanisms of foraging. Science 336:95–98.

Kolling N, Wittmann MK, Behrens TEJ, Boorman ED, Mars RB, Rushworth MFS (2016) Value, search, persistence and model updating in anterior cingulate cortex. Nat Neurosci 19:1280–1285.

Krajbich I, Armel C, Rangel A (2010) Visual fixations and the computation and comparison of value in simple choice. Nat Neurosci 13:1292–1298.

Krauzlis RJ, Bollimunta A, Arcizet F, Wang L (2014) Attention as an effect not a cause. Trends Cogn Sci 18:457–464.

Kriegeskorte N, Mur M, Ruff DA, Kiani R, Bodurka J, Esteky H, Tanaka K, Bandettini PA (2008) Matching categorical object representations in inferior temporal cortex of man and monkey. Neuron 60:1126–1141.

Kriegeskorte N, Simmons WK, Bellgowan PSF, Baker CI (2009) Circular analysis in systems neuroscience: the dangers of double dipping. Nat Neurosci 12:535–540.

Luyckx F, Nili H, Spitzer B, Summerfield C (2019) Neural structure mapping in human probabilistic reward learning. Elife 8:e42816.

Markant D, Gureckis TM (2012) Does the utility of information influence sampling behavior? Proc Annu Conf Cogn Sci Soc 34:719–724.

Milosavljevic M, Malmaud J, Huth A, Koch C, Rangel A (2010) The drift diffusion model can account for the accuracy and reaction time of value-based choices under high and low time pressure. Judgm Decis Mak 5:437–449.

Monosov IE (2020) How outcome uncertainty mediates attention, learning, and decision-making. Trends Neurosci 43:795–809.

Navarro DJ, Newell BR, Schulze C (2016) Learning and choosing in an uncertain world: an investigation of the explore–exploit dilemma in static and dynamic environments. Cogn Psychol 85:43–77.

Neubert F, Mars RB, Sallet J, Rushworth MFS (2015) Connectivity reveals relationship of brain areas for reward-guided learning and decision making in human and monkey frontal cortex. Proc Natl Acad Sci U S A 112:E2695–E2704.

Newell A, Simon HA (1972) Human problem solving. Englewood Cliffs, NJ: Prentice-Hall.

Nili H, Wingfield C, Walther A, Su L, Marslen-Wilson W, Kriegeskorte N (2014) A toolbox for representational similarity analysis. PLoS Comput Biol 10:e1003553.

Op de Beeck HP (2010) Against hyperacuity in brain reading: spatial smoothing does not hurt multivariate fMRI analyses? NeuroImage 49:1943–1948.

O'Toole AJ, Jiang F, Abdi H, Haxby JV (2005) Partially distributed representations of objects and faces in ventral temporal cortex. J Cogn Neurosci 17:580–590.

Payne JW (1976) Task complexity and contingent processing in decision making: an information search and protocol analysis. Organ Behav Hum Perform 16:366–387.

Pisauro MA, Fouragnan E, Retzler C, Philiastides MG (2017) Neural correlates of evidence accumulation during value-based decisions revealed via simultaneous EEG-fMRI. Nat Commun 8:15808.

Pochon JB, Riis J, Sanfey AG, Nystrom LE, Cohen JD (2008) Functional imaging of decision conflict. J Neurosci 28:3468–3473.

Quilodran R, Rothé M, Procyk E (2008) Behavioral shifts and action valuation in the anterior cingulate cortex. Neuron 57:314–325.

Ratcliff R, McKoon G (2008) The diffusion decision model: theory and data for two-choice decision tasks. Neural Comput 20:873–922.

Rodriguez CA, Turner BM, Van Zandt T, McClure SM (2015) The neural basis of value accumulation in intertemporal choice. Eur J Neurosci 42:2179–2189.

Sallet J, Mars RB, Noonan MP, Neubert F-X, Jbabdi S, O'Reilly JX, Filippini N, Thomas AG, Rushworth MF (2013) The organization of dorsal frontal cortex in humans and macaques. J Neurosci 33:12255–12274.

Sepulveda P, Usher M, Davies N, Benson A, Ortoleva P, De Martino B (2020) Visual attention modulates the integration of goal-relevant evidence and not value. eLife 9:e60705.

Shadlen MN, Shohamy D (2016) Decision making and sequential sampling from memory. Neuron 90:927–939.

Smith S, Nichols T (2009) Threshold-free cluster enhancement: addressing problems of smoothing, threshold dependence and localisation in cluster inference. NeuroImage 44:83–98.

Smith SM (2002) Fast robust automated brain extraction. Hum Brain Mapp 17:143–155.

Smith SM, Krajbich I (2019) Gaze amplifies value in decision making. Psychol Sci 30:116–128.

Stewart N, Hermens F, Matthews WJ (2016) Eye movements in risky choice: eye movements in risky choice. J Behav Decis Mak 29:116–136.

Stoll FM, Fontanier V, Procyk E (2016) Specific frontal neural dynamics contribute to decisions to check. Nat Commun 7:11990.

Talluri BC, Urai AE, Tsetsos K, Usher M, Donner TH (2018) Confirmation bias through selective overweighting of choice-consistent evidence. Curr Biol 28:3128–3135.e8.

Thompson KG, Bichot NP (2005) A visual salience map in the primate frontal eye field. Prog Brain Res 147:251–262.

Usher M, McClelland JL (2001) The time course of perceptual choice: the leaky, competing accumulator model. Psychol Rev 108:550–592.

Venkatraman V, Rosati AG, Taren AA, Huettel SA (2009) Resolving response, decision, and strategic control: evidence for a functional topography in dorsomedial prefrontal cortex. J Neurosci 29:13158–13164.

Wessel JR, Danielmeier C, Morton JB, Ullsperger M (2012) Surprise and error: common neuronal architecture for the processing of errors and novelty. J Neurosci 32:7528–7537.

White JK, Bromberg-Martin ES, Heilbronner SR, Zhang K, Pai J, Haber SN, Monosov IE (2019) A neural network for information seeking. Nat Commun 10:5168.

Wunderlich K, Rangel A, O'Doherty JP (2009) Neural computations underlying action-based decision making in the human brain. Proc Natl Acad Sci 106:17199–17204.

Zhang J, Hughes LE, Rowe JB (2012) Selection and inhibition mechanisms for human voluntary action decisions. NeuroImage 63:392–402.